



# Generation of positrons via pair-creation from Compton scattered gamma-rays

K. Dobashi<sup>a,\*</sup>, T. Hirose<sup>a</sup>, T. Kumita<sup>a</sup>, Y. Kurihara<sup>b</sup>, T. Muto<sup>a</sup>, T. Omori<sup>b</sup>,  
T. Okugi<sup>a</sup>, K. Sugiyama<sup>a</sup>, J. Urakawa<sup>b</sup>

<sup>a</sup>*Department of Physics, Tokyo Metropolitan University, 1-1 Minamiohsawa Hachioji-shi, Tokyo 192-0397, Japan*

<sup>b</sup>*KEK High Energy Accelerator Research Organization, 1-1 Oho, Tsukuba-shi, Ibaraki 305-0801, Japan*

Received 11 November 1998; received in revised form 6 June 1999; accepted 12 June 1999

## Abstract

An important role of positron ( $e^+$ ) polarization in future linear colliders is discussed in terms of effective polarization, which is closely related to the clear observation of interesting reaction processes in  $e^-e^+$  collisions. In order to verify our proposed method, in which highly polarized  $e^+$  can be generated through Compton scattering of laser light off a relativistic electron ( $e^-$ ) beam, we performed an experiment to prove the principle and observed  $e^+$  productions for the first time. It was found that the production rates of  $e^+$  are not only consistent with those of  $e^-$  and  $\gamma$ -ray but also in good agreement with numerical estimations. © 1999 Published by Elsevier Science B.V. All rights reserved.

## 1. Introduction

It is generally understood that for a future electron ( $e^-$ )-positron ( $e^+$ ) collider,  $e^-$  polarization is useful in order to investigate the details of the standard model by enhancing certain types of interactions or by suppressing dominant backgrounds due to the reaction process  $e^-e^+ \rightarrow W^-W^+$ . Within the framework of the standard model, high-energy  $e^-$  and  $e^+$ , which annihilate each other, are always in their combination of  $e_L^-e_R^+$  or  $e_R^-e_L^+$  with the suffix L(R) representing a left(right)-handed helicity. Thus, it may be considered that if only an  $e^-$  is polarized,  $e^+$  helicity is automatically

determined as opposite to that of the  $e^-$ . In the following, we simply denote only L or R for  $e^-e^+$  collisions. It is well known that if right-handed helicity is chosen for an  $e^-$ , thus leading to the combination R–L, contribution of  $W^-W^+$  production are highly suppressed. Since in many cases, the  $W^-W^+$  process causes serious backgrounds, the suppression of this process offers a favorable circumstance to observe exotic processes, which usually have small production cross sections. However, since the magnitude of  $e^-$  polarization is not 100%, another combination L–R is necessarily mixed into the combination R–L, and the ability to suppress backgrounds is thus deteriorated. This difficulty can be overcome by polarizing  $e^+$  as well as  $e^-$ . Indeed, we have pointed out the important role of  $e^+$  polarization to examine details of the standard model and exotic phenomena beyond the standard model [1–4].

\*Corresponding author.

E-mail address: kdobashi@phys.metro-u.ac.jp (K. Dobashi)

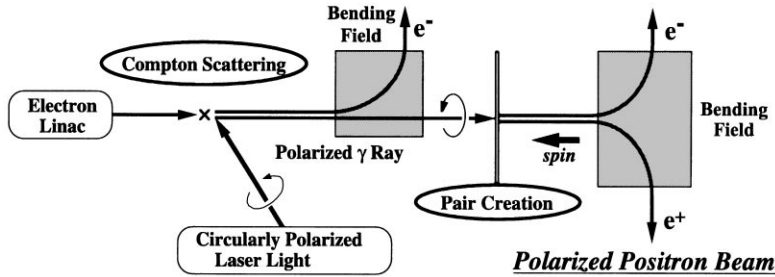


Fig. 1. Schematic illustration of a polarized positron source via Compton scattering of circularly polarized laser beam off relativistic  $e^-$  beam.

Recent progress made on semiconductor photocathodes has attained the development of high-intensity polarized  $e^-$  beam with a polarization greater than 70% [5–7], while the development of polarized  $e^+$  beam with sufficient intensity and magnitude of polarization encounters numerous technical difficulties because  $e^+$  must be artificially created. In 1996, we proposed a new method [8], in which the Compton scattering of circularly polarized laser beam off a relativistic  $e^-$  beam permits the creation of polarized  $\gamma$ -rays, which, in the subsequent pair-creation process, creates highly polarized  $e^+$ s, as illustrated in Fig. 1. To verify this method, we designed an experiment by generating a polarized  $e^+$  and measuring the  $e^+$  polarization in the successive three quantum processes, i.e., Compton scattering, pair creation, and Bhabha scattering. In the present experiment, as a first step, we observed  $\gamma$ -rays and  $e^+$ s using a 1.26 GeV  $e^-$  beam and a non-polarized laser beam.

The future linear collider JLC requires an extremely high intensity  $e^+$  beam with a complicated multi-bunch structure [9]. In compliance with our method, we have designed a JLC polarized  $e^+$  source [10–15]. In 1979, Balakin and Mikhailichenko had proposed the method of producing polarized  $\gamma$ -rays by utilizing a high intensity  $e^-$  beam of about 150 GeV, which propagated through a long helical undulator of about 150 m [16,17]. It should be emphasized that our proposed system is relatively compact as well as based on well-understood QED processes. Therefore, it ensures reliable estimations of the production rates and the magnitude of  $e^+$  polarization, even though there still remain several technically challenging problems with respect

to a high intensity  $e^-$  linac and multi-laser systems [14] as well as achievement of efficient collisions of electron and laser beams.

In Section 2, we discuss the roles of  $e^+$  polarization in terms of an effective polarization, a transverse polarization, and some considerations relating to physics requirements. Section 3 presents the first results of observing  $e^+$  production on the basis of the proposed method of laser-Compton scattering. In Section 4, various properties of  $e^-$  and laser beams are described, and the luminosity of the laser- $e^-$  collision is derived so as to compare the data with the numerical predictions. Section 5 is devoted to conclusions and future prospects.

## 2. Roles of positron polarization

As is well known, the effective polarization  $P_{\text{eff}}$  at  $e^-e^+$  collisions is defined as

$$P_{\text{eff}} = \frac{P_1 - P_2}{1 - P_1 P_2} \quad (1)$$

where  $P_1$  and  $P_2$  stand for the  $e^-$  and  $e^+$  beam polarizations, respectively:  $P_1 = 1$  ( $P_2 = -1$ ) represents 100% polarization for a right-handed  $e^-$  beam (a left-handed  $e^+$  beam). It is understood from Eq. (1) that  $P_{\text{eff}}$  can be significantly improved if an  $e^+$  beam as well as an  $e^-$  beam is polarized [18,19]. Here assuming that errors of measuring the polarization both for  $e^-$  and  $e^+$  beams are 1% and the  $e^-$  beam has the polarization of 90%, we obtain  $P_{\text{eff}}$  and its error  $\Delta P_{\text{eff}}/P_{\text{eff}}$  as a function of

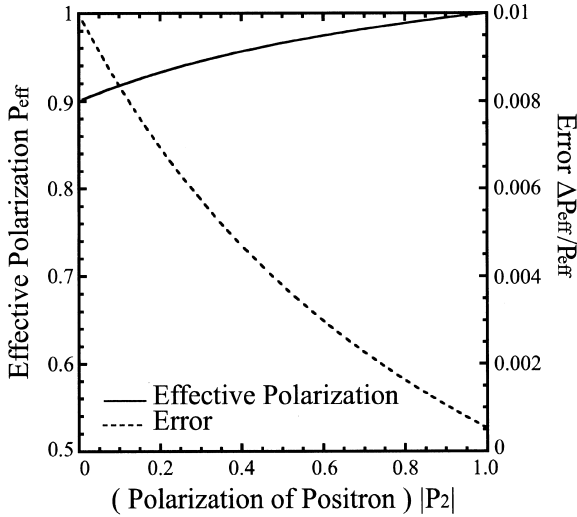


Fig. 2. Effective polarization  $P_{\text{eff}}$  and its relative errors  $\Delta P_{\text{eff}}/P_{\text{eff}}$  as a function of  $e^+$  polarization  $P_2$ . Here it is assumed that errors of measuring the polarization both for  $e^-$  and  $e^+$  beams are 1% and the  $e^-$  beam has the polarization of 90%.

the  $e^+$  polarization shown in Fig. 2. For example, if  $P_2 = -80\%$  in addition to  $P_1 = 90\%$  is achieved, we can obtain the high value of  $P_{\text{eff}} = 99\%$  and the considerably small error  $\Delta P_{\text{eff}}/P_{\text{eff}} = 0.0016$ , which can help us to measure some physical parameters very precisely as compared with the case of only  $e^-$  polarization  $P_1 = 90\%$ . The  $e^+$  polarization also significantly enhances the signal-to-noise ratio in the case of observing new particles.

Furthermore, some models beyond the standard model predict interesting processes emerging in R–R or L–L combination of helicities. For example, pair production of a selectron  $\tilde{e}^-$  and a stop squark  $\tilde{t}^+$  through a neutralino  $\tilde{\chi}^0$  exchange diagram predicted by a super-symmetry model can be efficiently observed via the R–R combination of beam polarizations. It is expected that the strong suppression of the fermion pair ( $\text{ff}$ ) production as well as the  $W^-W^+$  production through annihilation diagrams is accomplished.

The importance of transverse polarization was also pointed out [20]: If both  $e^-$  and  $e^+$  have the transverse polarization which is described as a linear combination of longitudinal polarizations, un-

known phenomena emerging in the R–R or L–L combinations might be enhanced by the allowed processes, through interference between different combinations of longitudinal polarizations of  $e^-$  and  $e^+$ , i.e., R–R and L–R (R–L) or L–L and L–R (R–L). Consequently, the controllability of the spins of an initial  $e^+$  beam as well as an  $e^-$  beam should be of great importance in a linear collider experiment where new phenomena can be clearly observed.

### 3. Experimental

#### 3.1. Differential cross sections

We attempted to calculate various quantities that are necessary for designing experimental facilities to observe production and polarization of positrons. Utilizing GRACE [21], we calculate the differential cross section of the Compton scattering process, in which circularly polarized laser beam of 2.33 eV with a helicity  $h = 1$  are scattered by an unpolarized  $e^-$  beam of 1.26 GeV. Fig. 3 shows (a) the differential cross section and (b) the polarization for Compton scattered  $\gamma$ -rays as a function of the  $\gamma$ -ray energy. As seen in Fig. 3, high degree of polarization (helicity  $h = -1$  in this case) is expected for the back scattered  $\gamma$ -rays near the high-energy end of the spectrum. The total cross section of Compton scattering is estimated to be 637 mb. Using the energy and polarization distributions given in Fig. 3, we calculated the differential cross section of pair-creation and the  $e^+$  polarization as shown in Fig. 4: The calculation based on the helicity amplitude was performed numerically using GRACE. Fig. 4 indicates that the polarization of 80% can be achieved, if  $e^+$ s with the energy higher than 23 MeV are selected. Since the cross section of pair-creation is proportional to the square of the charge number of a nucleus,  $Z^2$ , we present the cross section normalized by  $Z^2$  in the Fig. 4. On the other hand, the ionization energy loss of  $e^+$  per nucleus is, roughly speaking, proportional to the charge number  $Z$ . Consequently, a material with a large  $Z$  is suitable as the target material, and thus, we adopt a thin tungsten (W) target.

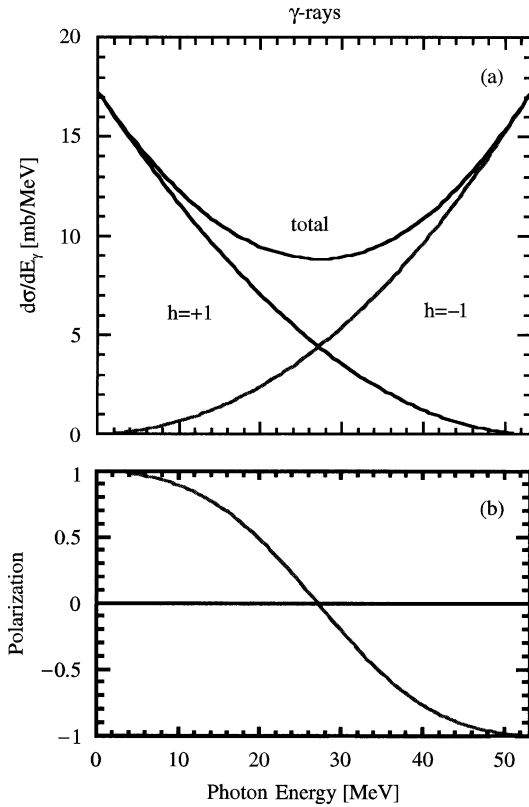


Fig. 3. (a) Differential cross section of circularly polarized laser beam of 2.33 eV with a helicity  $h = 1$  scattered by an unpolarized  $e^-$  beam of 1.26 GeV. Here  $h = +1(-1)$  represents a positive (negative) helicity. The “total” shows the sum of them. (b)  $\gamma$ -ray polarization as a function of the  $\gamma$ -ray energy.

### 3.2. Apparatus and data taking

A schematic view of the experimental set-up [22,23] is depicted in Fig. 5. Extracted  $e^-$  beam of 1.26 GeV/c with the intensity  $N_{e^-} = 6 \times 10^9$   $e^-$ /bunch and the time width 20 ps are provided every 1.28 s from the ATF damping ring [24], which has been constructed as a test facility for the linear collider JLC. We used a pulse-laser, Nd:YAG laser, Continuum NY81C-10 with the total energy of 200 mJ at the wavelength of 532 nm (the second harmonic). In the present experiment, as a first step to prove the principle of our method, we did not measure the  $e^+$  polarization but verify the  $e^+$  production rate. Hence, non-circularly-polarized laser beam is guided from the laser generator,

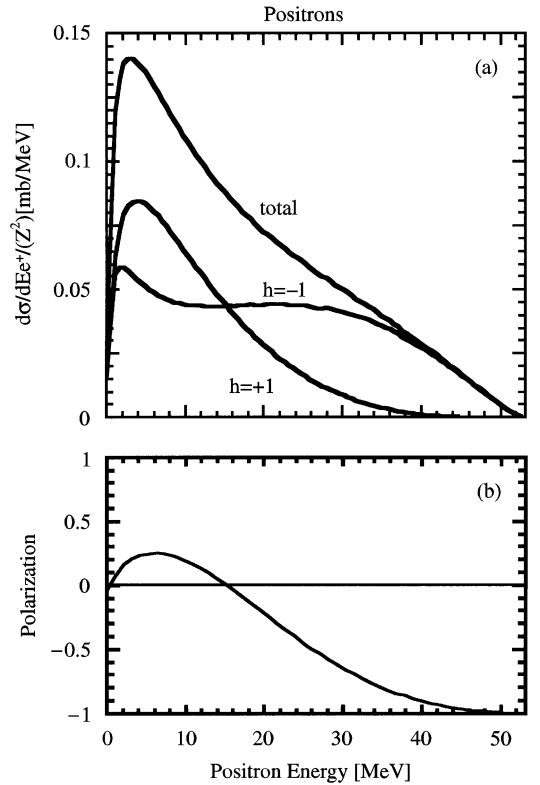


Fig. 4. (a) Differential cross section of pair-creation as a function of the  $e^+$  energy. The cross section is normalized by the square of a charge number of a nucleus  $Z^2$ . Here  $h = +1(-1)$  represents a positive (negative) helicity. (b)  $e^+$  polarization as a function of the  $e^+$  energy.

which is set outside a radiation shield, to a collision point after reflections on the five mirrors located in air as shown in Fig. 5 and a small prism located in the vacuum of the beam pipe. Since the laser beam travels through one prism, two lenses and one sapphire-window and is reflected on five mirrors, the laser intensity is reduced to 65%, thus 130 mJ at the collision point and the focal length for this optics becomes rather long, i.e., 454 cm. A crossing angle between  $e^-$  and laser beams is  $\varphi = 7$  mrad.

Immediately after Compton scattering, an initial  $e^-$  beam is bent away by means of a bending magnet and then, back scattered  $\gamma$ -rays are injected on the 1 mm thick W-target to pair-create  $e^-$ s and  $e^+$ s. A pair of magnets called “the separation-magnet”, specially designed to separate  $e^+$ s from

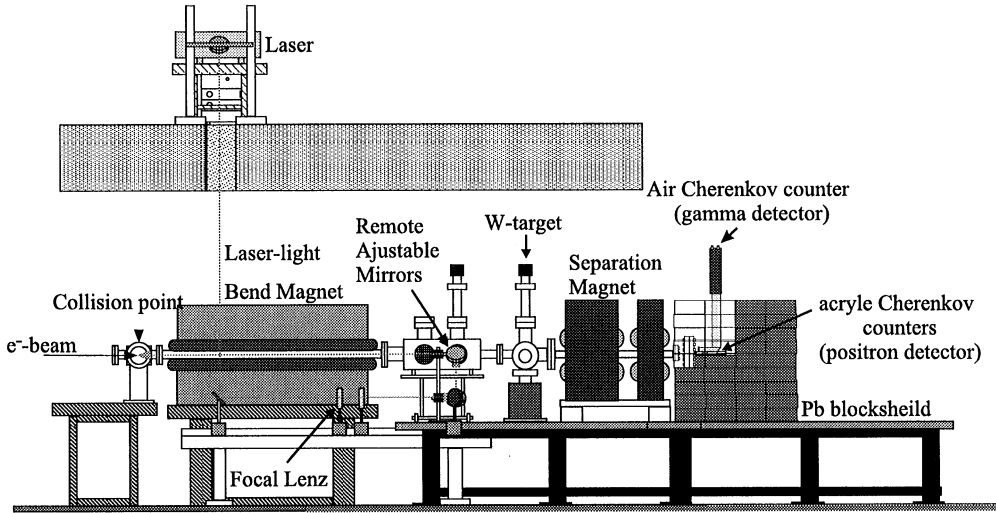


Fig. 5. Side view of the experimental set-up for the measurement of generated  $e^+$ s and  $\gamma$ -rays.

Table 1

Transportation efficiency of the separation magnet, expected numbers of  $e^+$ s traveling through the magnet and those observed by the detector as a function of the magnet current. Detected numbers of  $e^+$ /bunch are also given

Magnet current (A):	14	16	18	20
Transportation efficiency	0.019	0.017	0.013	0.010
Expected no. of $e^+$ s at the exit of the magnet	4.39	3.92	3.00	2.30
Expected no. of observed $e^+$ s	1.04	0.93	0.71	0.54
Detected no. of $e^+$ s (experimental)	$1.13 \pm 0.04$	$0.93 \pm 0.03$	$0.75 \pm 0.03$	$0.66 \pm 0.02$

$e^-$ s, is located just after the W-target. The separation magnet effectively separates  $e^+$ s with the energy higher than about 23 MeV, so as to yield highly polarized  $e^+$ s. The target thickness was determined to compromise following two conditions. First, the production rate of  $e^+$ s increases with the target thickness. On the other hand, the  $e^+$  transportation efficiency through the separation-magnet decreases when a thick target is employed, because the effect due to multiple scattering of the produced  $e^+$ s in the target material increases with the target thickness. The appropriate target thickness was estimated as 1 mm using the simulation program EGS4 [25] for electromagnetic interactions of charged particles in the W target. The  $e^+$  transportation efficiency through the separation-magnet is estimated by Monte Carlo simulation as given in

Table 1 for magnet currents  $I = 14$ –20 A. Spin-flip effect in the target material was checked by modifying the EGS4 with the help of the HELAS utility [26] and found to be around 1%.

Since the experimental area was exposed to high backgrounds originating from the electron beam line, we made use of, for  $\gamma$ -ray measurement, an air Cherenkov counter with the refractive index of  $n = 1.0003$ . This counter is insensitive to charged particles with the kinetic energy below the threshold of 20.4 MeV. In a Pb-plate of 5 mm thicknesses placed at the entrance of the air Cherenkov counter, 60% of Compton scattered  $\gamma$ -rays are converted to  $e^-$ s and  $e^+$ s. One  $e^-$  and  $e^+$ , which have the kinetic energy well above the threshold, emit 0.48 Cherenkov photons per 10 mm. The size of an air Cherenkov counter is  $40 \times 50 \text{ mm}^2$  in cross

section and 100 mm in length. For  $e^+$  measurement, we adopted four acrylic Cherenkov counters with  $n = 1.48$  corresponding to the threshold energy 0.183 MeV. One  $e^+$  emits 447 Cherenkov photons per 10 mm leading to 59 photoelectrons on the photocathode. The size of an acrylic radiator is 10 mm in diameter and 50 mm in length.

The geometrical overlap of the laser beam with  $e^-$  beam was checked on a screen monitor by remote controlling the angles of two reflection mirrors, whose minimum pitch is about 100  $\mu$ rad, thus permitting to the adjustable precision of 52  $\mu$ m for the laser spot at the collision point. To synchronize the laser pulse and the  $e^-$  bunch, we utilize the timing signal from the master oscillator which controls the whole accelerator system. The  $Q$ -switch of the laser generator is triggered by the signal from the master oscillator through a digital delay module. Thus, the delay time is adjusted by comparing the timing of laser pulse observed with a photodiode at the exit of a laser generator with the timing signal from the beam position monitor located near the collision point. Finally, fine adjustment of determining the timing of a laser pulse is performed by maximizing the intensity of back scattered  $\gamma$ -rays. From the analysis of the time distribution of  $\gamma$ -rays thus measured, we derived the energy and the pulse duration of the laser pulses which are effectively utilized in the laser–electron interaction; the estimated magnitude of the effective laser energy is 15.6% resulting in the effective energy of 20.3 mJ for the laser pulse duration of  $\sigma = 0.27$  ns.

To suppress systematic errors due to long-term variation of the related parameters of the accelerator, laser systems, detectors and electronics, we switched on and off the laser beam alternatively to each  $e^-$  bunch and measure the pulse height (ADC counts) of the Cherenkov counters. Since the ADC count of an air Cherenkov counter is proportional to the sum of back scattered  $\gamma$ -rays and machine-related background, there should be a sharp peak in the laser-off signal at the 0 ADC count if no background emerges. Indeed, Fig. 6(a) indicates the relatively narrow laser-off peak which is separated well from the laser-on distribution corresponding to  $\gamma$ -ray production. In a similar manner,  $e^+$  signals were observed as shown in Fig. 6(b). Unfortunately,  $e^+$  detectors are subject to large backgrounds

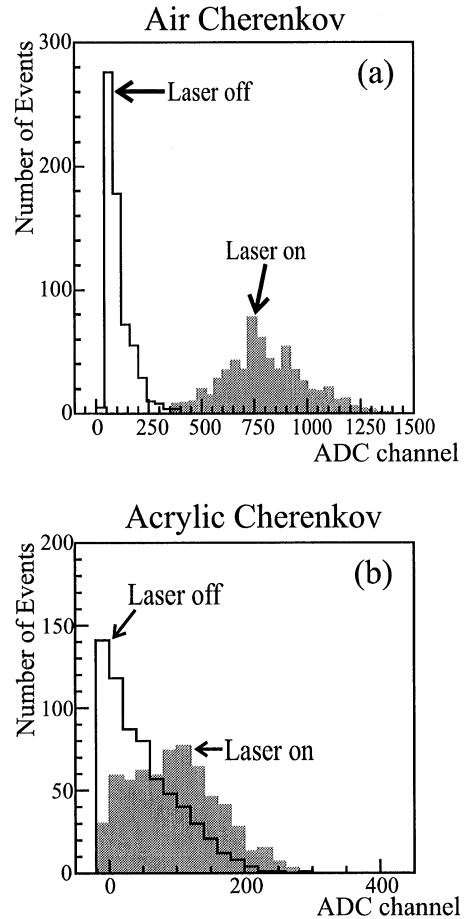


Fig. 6. Number of events as a function of pulse height (ADC counts) for (a) the detection of  $\gamma$ -rays with an air Cherenkov counter and for the detection of  $positron$  with (b) an acrylic Cherenkov counter. Shaded (white) histograms show events with laser-on (laser-off).

because acrylic Cherenkov counters have a lower threshold and thus, a large overlap between the laser-on and laser-off signals is observed. Using  $\pi^-$  beam of 2 GeV/c provided from the proton synchrotron at KEK, we calibrated the acrylic Cherenkov counters. Then we derived a number of generated  $e^+$ s from the difference between laser-on and laser-off signals. The number of observed  $e^+$ s per bunch as a function of the current of the separation magnet is shown in Fig. 7. In order to confirm the reliability of our measuring system,  $e^-$ s were also observed by reversing the polarity of the

separation-magnet. The number of observed  $e^-$ s per bunch is  $0.73 \pm 0.02$  for  $I = 18$  A, which is in good agreement with the number of  $e^+$ s per bunch for  $I = 18$  A, i.e.,  $0.75 \pm 0.03$ . Furthermore, it was checked that no difference was observed between laser-on and laser-off signals, when the W-target was removed.

#### 4. Numerical predictions

Horizontal and vertical emittances of the  $e^-$  beam were measured to be  $\varepsilon_x = 2.6 \times 10^{-9}$  rad m and  $\varepsilon_y = 6.5 \times 10^{-11}$  rad m, respectively. Using these values and a Twiss parameter  $\beta$  at the collision point, i.e.,  $\beta_x = 2.4$  m and  $\beta_y = 1.5 \times 10^2$  m, the vertical beam size was estimated as  $\sigma_{ye} = 97$   $\mu$ m. However, taking into account a dispersion  $\eta_x = 0.6$  m and a momentum spread  $\Delta p/p = 7.5 \times 10^{-4}$ , we obtain a much larger horizontal beam size  $\sigma_{xe} = 440$   $\mu$ m. The  $e^-$  bunch width 20 ps results in the longitudinal beam size of 6 mm. On the other hand, the laser beam size is  $\sigma_{xL} = 0.85$  mm and  $\sigma_{yL} = 1.0$  mm in the transverse direction, and  $\sigma_{zL} = 8.1$  cm in the longitudinal direction. Assuming a Gaussian beam shape both for  $e^-$  and laser beams, the luminosity  $\mathcal{L}$  is represented as

$$\mathcal{L} = \frac{N_e N_L}{2\pi \sqrt{\sigma_{ye}^2 + \sigma_{yL}^2} \sqrt{\cos^2\left(\frac{\varphi}{2}\right)(\sigma_{xe}^2 + \sigma_{xL}^2) + \sin^2\left(\frac{\varphi}{2}\right)(\sigma_{ze}^2 + \sigma_{zL}^2)}} \quad (2)$$

where  $N_e = 6 \times 10^9$  is the  $e^-$  bunch population, and the number of laser photons in a laser pulse  $N_L = 5.4 \times 10^{16}$  can be obtained from the effective laser pulse energy 20.3 mJ at the collision point. Using the parameters of the  $e^-$  and laser beams given above, the luminosity for the laser- $e^-$  collision is calculated to be  $5.2 \text{ mb}^{-1}$ , which results in numbers of  $\gamma$ -rays generated through the collision, i.e.,  $3.3 \times 10^3/\text{bunch}$ . According to EGS4 simulations, the conversion efficiency from  $\gamma$ -rays to  $e^+$  on the W target of 1 mm thickness is obtained to be 7.0%, so that the total number of  $e^+$ s per one collision is predicted as  $2.3 \times 10^2/\text{bunch}$ . Using the transportation efficiency of the separation magnet,

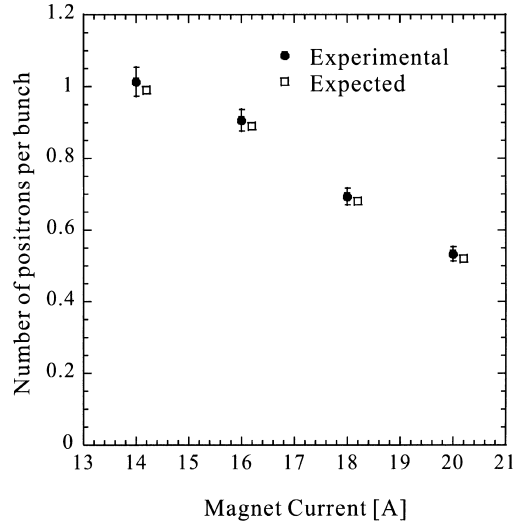


Fig. 7. Average numbers of detected  $e^+$ s per bunch for different current settings of the separation-magnet. Black circles represent experimental data and squares represent expectation values (see text). The predicted values are shifted slightly rightward for easiness of looking.

we estimate the number of  $e^+$ s at the exit of the separation magnet. Then, taking account of the acceptance 0.24 for the whole acrylic counters, we can predict the expected number of  $e^+$ s.

Table 1 summarizes experimental data and expected numbers of  $e^+$ s per bunch together with the transmission efficiency for the current  $I = 14, 16, 18, 20$ . Fig. 7 demonstrates, as a function of the current  $I$ , the measured and expected numbers of  $e^+$  per bunch, which look to be in good agreement with each other.

#### 5. Conclusions and future prospect

We observed  $e^+$  production for the first time via successive two quantum processes, i.e., Compton scattering and pair-creation, and confirmed that

the production rates of  $e^+$ s and  $e^-$ s are consistent with each other. Good agreement between the experimental data and the numerical estimation verifies that our proposed method is promising for generating polarized  $e^+$ s. It should be noted that our method is based on the well understood QED processes and thus further upgrading or improvement of facilities can be quantitatively estimated although there might be difficult but interesting problems in association with laser-beam interaction. Actually through the present experiment, we have accumulated numerous technical information on laser and  $e^-$  beams collisions, which helps to improve significantly the signal-to-noise (S/N) ratio for attaining our goal of measuring the  $e^+$  polarization by Bhabha scattering of  $e^+$  on a magnetized iron. Indeed, to measure the  $e^+$  polarization with good precision via successive three quantum processes, we are designing a special off-axis mirror to achieve head-on collision of laser and  $e^-$  beams as well as strong focusing of laser beam, so that the luminosity is significantly increased, thus leading to the improvement of the S/N ratio more than 100 times. Furthermore, fine tuning of the damping ring and adding lead shields to avoid backgrounds from the  $e^-$  beam line will be greatly helpful to achieve our final goal.

Future colliding experiments at JLC require extremely high intensity  $e^+$  beam, i.e.,  $7 \times 10^9/\text{bunch}$  with a highly complicated time-structure, a so-called multi-bunch beam. The conceptual design [4,14,27] indicates that our proposed method is also applicable to polarized  $e^+$  production at JLC, if a high-intensity  $e^-$  beam of  $10^{11}e^-/\text{bunch}$  and ultra-high energy multi-bunch laser beams are provided in Compton scatterings. The technical details on the realistic design are published in Refs. [14,27]. It should be remarked that, as discussed in Ref. [20], the transverse polarization in the collider experiment might be of great importance to reveal various new phenomena and thus, we have to measure three components of a polarization vector with reasonable accuracy. It was found that the method on the basis of laser-Compton scattering can be utilized again to determine both longitudinal and transverse polarizations by measuring the asymmetry of angular distributions of back scattered  $\gamma$ -rays [28]. Further discussions of

$e^\pm$  polarimetry at a linear collider will be given elsewhere.

## Acknowledgements

We would like to express our gratitude to all members of the ATF group for ATF operation. We are also indebted to the JLC calorimeter group for providing us an opportunity for counter calibration. In designing an off-axis mirror to improve the luminosity in the next step, we are extensively discussing with Drs. I. Ben Zvi, I.V. Pogorelski of BNL, and Dr. A. Tsunemi of SHI. This research was partially supported by a Research Fund of KEK for Cooperative Developments and a Grant-in-Aid for Scientific Research 10640294 from the Ministry of Education, Science, Sports and Culture of Japan.

## References

- [1] T. Hirose, in: A. Miyamoto Y. Fujii, T. Matsui, S. Iwata (Eds.), *Proceedings of the International Workshop on Physics and Experiments with Linear Colliders*, Morioka Iwate, 8–12 September 1995, World Science, Singapore, 1996, pp. 748–756.
- [2] M. Chiba et al., KEK Preprint 95-92, 1995.
- [3] T. Omori, *Proceedings of the International Workshop on New Kinds of Positron Sources for Linear Colliders*, SLAC-R-502, SLAC, March 4–7, 1997, p. 285.
- [4] T. Omori, talk given at The First ACFA Workshop on Physics/Detector at the Linear Collider, Tsinghua University, Beijing, The People's Republic of China, November 26–27, 1998, KEK-Preprint 98-237.
- [5] T. Omori, Y. Kurihara, T. Nakanishi, H. Aoyagi, T. Baba, T. Furuya, K. Itoga, M. Mizuta, S. Nakamura, Y. Takeuchi, M. Tsubata, M. Yoshioka, *Phys. Rev. Lett.* 67 (1991) 3291.
- [6] T. Nakanishi, H. Aoyagi, H. Horinaka, Y. Kamiya, T. Kato, S. Nakamura, T. Saka, M. Tsubata, *Phys. Lett. A* 158 (1991) 345.
- [7] T. Maruyama, E.L. Garwin, R. Preost, G.H. Zapalac, J.S. Smith, J.D. Wlker, *Phys. Rev. Lett.* 66 (1991) 2351.
- [8] T. Okugi, Y. Kurihara, M. Chiba, A. Endo, R. Hamatsu, T. Hirose, T. Kumita, T. Omori, Y. Takeuchi, M. Yoshioka, *Jpn. J. Appl. Phys.* 35 (1996) 3677.
- [9] JLC Design Study, KEK Report 97-1, 1997.
- [10] T. Omori, *Proceedings of the International Workshop on New Kinds of Positron Sources for Linear Colliders*, SLAC-R-502, SLAC, March 4–7, 1997, p. 341.



- [11] T. Omori, Seventh International Workshop on Linear Colliders, Zvenigorod, Russia, 1997, Working Group 2 <http://www.desy.de/conferences/LC97/proceed/lc97.htm>.
- [12] T. Hirose, Proceedings of the Second ATF International Collaboration Meeting, Tsukuba, June 1997, KEK Proceedings 97-7, 1997.
- [13] T. Hirose, Proceedings of the second Japan–US Workshop on Interaction of High Power Waves with Plasmas and Matters, Osaka, 1996, Inst. of Laser Engineering, Osaka University, 1996, p. 105.
- [14] T. Omori, K. Dobashi, T. Hirose, T. Kumita, Y. Kurihara, T. Okugi, K. Sugiyama, A. Tsunemi, M. Washio, Proceedings of the First Asian Particle Accelerator Conference, KEK, March 23–27, 1998, KEK Preprint 98-13, TMU HEP/EXP 98-10.
- [15] T. Hirose, Talk given at International Conference on Laser'98, Tucson, AZ, USA, December 7–11, 1998. Preprint of Tokyo Metropolitan University, TMU HEP/EXP 99-1, 1999.
- [16] V.E. Balakin, A.A. Michailichenko, Preprint INP 79-85, 1979.
- [17] A.A. Michailichenko, Proceedings of the International Workshop on  $e^-e^+$  Sources and Pre-Accelerators for Linear Colliders (SOURCES '94), Schwerin, Germany, 1994, DESY 1994, p. 61.
- [18] K. Flöttman, DESY 95-064.
- [19] K. Fujii, T. Omori, KEK Preprint 95-127, 1995.
- [20] K. Hikasa, Phys. Rev. D 33 (1986) 3203.
- [21] Minami-Tateya-Collab., KEK-Report 92-19, 1992.
- [22] T. Hirose, Seventh International Workshop on Linear Colliders, Zvenigorod, Russia, 1997, Working Group <http://www.desy.de/conferences/LC97/proceed/lc97.htm>.
- [23] T. Hirose, Proceedings of The First Asian Particle Accelerator Conference KEK, March 23–27, 1998.
- [24] ATF Design and Study Report, KEK Internal 95-4, 1995.
- [25] W.R. Nelson, H. Hirayama, D.W.O. Rogers, SLAC-R-265.
- [26] K. Hagiwara, H. Murayama, I. Watanabe, KEK-Report 91-11, 1992.
- [27] A. Tsunemi et al., Joint ICFA/JAERI-kansai International Workshop on Second Generation Plasma Accelerators, Kansai Univ., July 14–18, 1997.
- [28] H. Ishiyama et al., KEK Preprint 96-141, Preprint of Tokyo Metropolitan University TMU HEP/EXP 96-10, 1996.